Ab Initio Molecular Orbital Study of the N(^{2}D) + HCN($^1\Sigma$) Reaction

Yuzuru Kurosaki* and Toshiyuki Takayanagi

Advanced Science Research Center, Japan Atomic Energy Research Institute, Tokai-mura, Naka-gun, Ibaraki 319-1195, Japan

Received: June 23, 1999

Ab initio MO calculations have been carried out for the N(^{2}D) + HCN($^1\Sigma$) reaction system. The CASSCF-(9,9)/cc-pVDZ level of theory was employed for initial processes, and addition of N(^{2}D) to the N atom was found to be energetically the most favorable pathway. Several intermediates and transition states located on overall reaction pathways except for the initial processes were optimized at the MP2(full)/cc-pVTZ level and their single-point energies were calculated at the PMP4(SDTQ,full)/cc-pVTZ level. It was found that the main product channel is CH($^2\Pi$) + N_2($^1\Sigma_g$), which is 53.1 kcal mol^{-1} lower in energy than the N(^{2}D) + HCN($^1\Sigma$) reactants.

1. Introduction

Reactions of electronically metastable atomic nitrogen N(^{2}D) with nitrile compounds are thought to be important processes in the chemistry of planetary atmosphere. In recent years, Titan's atmosphere has received considerable attention due to the Voyager observations that have provided detailed information of the atmospheric constituents.[1−3] It was revealed that the atmosphere includes several nitrile species such as HCN, HC_3N, and CH_3CN, as well as large amount of hydrocarbons. The source of nitrogen in the nitrile compounds is considered to be molecular nitrogen N_2, which is known to be a major atmospheric constituent. Although N_2 is chemically inactive, N_2^+, N(^{4}S), and N(^{2}D) can be produced from N_2 through electron impact, extreme-ultraviolet photolysis, and galactic-cosmic-ray absorption. In particular, electronically metastable atomic nitrogen, N(^{2}D), is thought to play major roles in the formation of nitrile compounds since it is known that N(^{2}D) is highly active as compared to electronically ground-state nitrogen N(^{4}S). Therefore it is likely that nitrile compounds in Titan's atmosphere are produced from reactions of N(^{2}D) with hydrocarbons such as CH_4, C_2H_6, C_2H_4, and C_2H_2, which are rich species in the atmosphere. As a consequence, reactions of N(^{2}D) with nitrile compounds should also become important chemical processes in Titan's atmosphere. Therefore it is necessary to theoretically examine the mechanism of reactions of N(^{2}D) with nitrile compounds in order to understand better the chemistry of Titan's atmosphere.

To date, experimental information on the mechanisms of the N(^{2}D) reactions have been quite limited since the reaction products have not been directly detected. For example, Fell et al.[4] measured overall rate constants for the reactions of N(^{2}D) with H_2, O_2, CO_2, CH_4, CF_4, etc.; however, since the reaction products were totally unidentified, the reaction mechanisms have remained almost unclear. In fact, it is not until quite recently that two research groups have developed advanced experimental techniques that can allow the study of the N(^{2}D) reactions under the single-collision condition. Umemoto and co-workers[5−9] have developed a laser photolysis technique and detected the NH radical as a product in the reactions of N(^{2}D) with H_2, H_2O, and saturated hydrocarbons. They also succeeded in measuring the nascent rotational and vibrational distributions of the NH radical; this dynamical information should give a clue to understanding the N(^{2}D) reaction mechanism. Casavecchia and co-workers[10] have developed a crossed beam scattering technique and detected the HCCN radical as a product of the N(^{2}D) + C_2H_2 reaction. Their results strongly support the hypothesis of Yung et al.[1,2] that explains the origin and role of the HCCN radical in Titan's atmosphere. Very recently, they[11] have measured the angular and velocity distribution of the ND molecule produced from the N(^{2}D) + D_2 reaction; the experimental results were found to be in good agreement with the theoretical predictions of the quasiclassical trajectory study.[11]

On the theoretical side, studies of the N(^{2}D) reactions have not been reported for many years; one of the reasons for this may be a difficulty in the electronic-state calculation. Since the electronic state of N(^{2}D), which is 5-fold degenerate without considering the spin−orbit interacton, is in an open-shell doublet state, a high multiconfigurational character should occur in the electronic state. Therefore, the potential energy surface for interaction in the initial stage cannot be described by the usual theoretical methods that are based on the single-determinant Hartree−Fock (HF) approximation. Very recently, however, we have carried out ab initio molecular orbital (MO) calculations for several N(^{2}D) reactions: N(^{2}D) + CH_4,[12,13] N(^{2}D) + C_2H_4,[14] N(^{2}D) + C_2H_2,[15] and N(^{2}D) + H_2O,[16] where complete active space self consistent field (CASSCF) or first-order configuration−interaction (FOCI) methods were employed for the initial processes. We have thus succeeded in predicting the initial reaction pathways of the N(^{2}D) reactions. Although the computational levels employed for the initial processes are still qualitative, we believe that the calculations have provided valuable information for the reaction mechanism and should be an important first step for quantitative discussion. It should also be noted that dynamics calculations based on the quasiclassical trajectory method for the N(^{2}D) reactions have recently been performed; however, they are still limited to the simplest system: N(^{2}D) + H_2[17−19] or N(^{2}D) + D_2.[11] Very recently, we have carried out ab initio classical trajectory calculations for the N(^{2}D) + CH_4 insertion reaction[20] and obtained valuable dynamics information.

* Corresponding author e-mail address: kurosaki@apr.jaeri.go.jp. Present address: Advanced Photon Research Center, Japan Atomic Energy Research Institute, Umemidai, Kizu-cho, Soraku-gun, Kyoto 619-0215, Japan.

10.1021/jp9920848 CCC: $18.00
Published on Web 11/03/1999

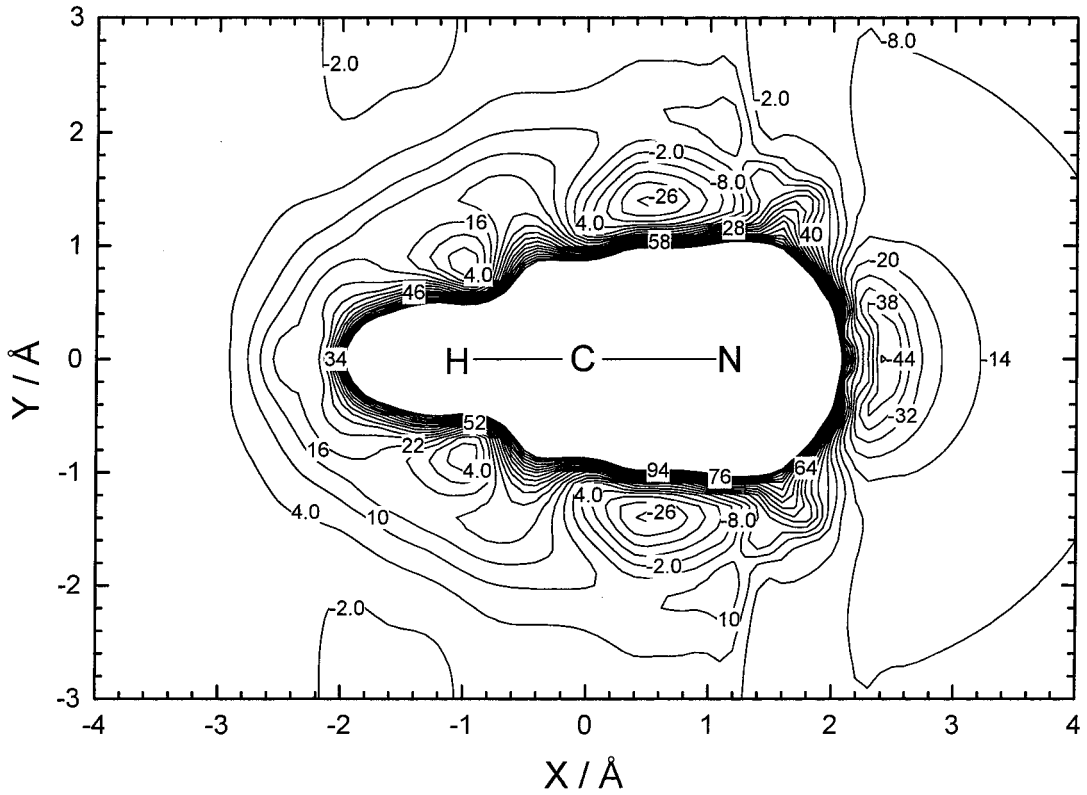

Figure 1. Contour map of the CASSCF(9,9)/cc-pVDZ potential energy surface for initial processes as a function of the N(^{2}D) position. Relative energy values with respect to the N(^{2}D) + HCN($^1\Sigma$) asymptote are given in kcal mol^{-1}. The HCN molecule is fixed to be the CASSCF(6,6)/cc-pVDZ geometry: d(C−H) = 1.0851 Å and d(C−N) = 1.1589 Å.

Our previous studies[12−16] have qualitatively revealed the initial processes of the N(^{2}D) reactions with hydrocarbon molecules (CH_4, C_2H_4, and C_2H_2) and H_2O. In the reaction with CH_4, two reaction pathways can be considered as the initial processes: insertion into the CH bond and abstraction of H. It was calculated[12] that insertion is more likely to occur than abstraction, which leads to the formation of an intermediate, CH_3NH. In the reaction with C_2H_4, three pathways can be thought of as the initial processes: addition to the CC π bond, insertion into the CH bond, and abstraction of H. The ab initio MO results predicted[14] that addition is energetically the lowest reaction pathway. In the reaction with C_2H_2, the same three pathways as those in the N(^{2}D) + C_2H_4 reaction are possible and addition to the CC π bond was again calculated[15] to be the lowest reaction pathway. Thus these results have led us to conclude that for saturated hydrocarbon molecules N(^{2}D) is likely to insert into the CH bond and for unsaturated hydrocarbon molecules N(^{2}D) is likely to add to the CC π bond. In the reaction with H_2O, three reaction pathways, addition to O, insertion into the OH bond, and abstraction of H, are possible as the initial processes. It was predicted[16] that addition to O is the most favorable pathway; however, an intermediate H_2ON produced via addition of N(^{2}D) to O was shown to easily isomerize into a very stable intermediate HNOH with a barrier height being only a few kcal mol^{-1} s. Therefore it could be said that insertion into the OH bond is the most favorable.

It is interesting to examine the interaction between N(^{2}D) and the CN triple bond of nitrile compounds and to compare to the computational results of hydrocarbons and H_2O described above. In this paper, we study the reaction with the simplest nitrile compound, N(^{2}D) + HCN($^1\Sigma$), using ab initio MO methods. Results are reported not only for the initial processes but also for the overall processes including intermediate minima, transition states (TSs), and final products. We believe that the present theoretical study provides valuable information for various fields of chemistry including N(^{2}D) reactions as well as for the chemistry of Titan's atmosphere.

2. Methods of Calculation

Ab initio MO calculations in this work were carried out using the HONDO7[21] program for the potential surface calculation and using the GAUSSIAN 94 program[22] for the geometry optimization and single-point energy calculation. For the initial processes the contour map for the potential energy surface was obtained at the CASSCF level, where nine electrons were distributed in the nine active orbitals (CASSCF(9,9)), with the correlation consistent valence double-ζ (cc-pVDZ) basis set of Dunning.[23] The active space includes three N 2p orbitals, CH σ and CH σ* orbitals, and two sets of CN π and CN π* orbitals. For overall reaction pathways except for the initial processes the second-order Møller−Plesset perturbation (MP2(full)) method[24−26] with the cc-pVTZ basis set[23] was used and several minima (M1-M6) and TSs (TS1-TS5) were optimized. Geometries of several fragments produced as final products of the N(^{2}D) + HCN reaction were also optimized at the same level of theory. Note that the MP calculations in this study are based on spin-restricted and spin-unrestricted Hartree−Fock (RHF and UHF) wave functions for closed-shell and open-shell molecules, respectively. Harmonic vibrational frequencies were computed analytically at the MP2(full) level,[27] and the optimized geometries were characterized as potential minima or saddle points. Single-point calculations for the optimized geometries were also carried out using the MP4(SDTQ,full)[28,29] method with the cc-pVTZ basis set. Since spin-unrestricted MPn (UMPn) wave functions for open-shell molecules are in general not the eigenfunctions of spin operator $\mathbf{S}^2$, spin-projected UMPn (PMPn) wave functions[30] were calculated and the spin contamination was completely removed.

3. Results and Discussion

A. Potential Energy Surface for Initial Processes. Figure 1 shows the contour map for the potential energy surface of the lowest doublet state of the $N(^2D) + HCN(^1\Sigma)$ system calculated at the CASSCF(9,9)/cc-pVDZ level as a function of the $N(^2D)$ position. The total energy of the $N(^2D) + HCN(^1\Sigma)$ asymptote was set to be the zero point of potential energy. During the calculation, the HCN geometry was fixed to be the CAS(6,6)/cc-pVDZ geometry: $d(C-H) = 1.0851$ Å and $d(C-N) = 1.1589$ Å.

The following four reaction pathways are possible in the initial step of the present reaction: abstraction of H, insertion into the CH σ bond, addition to the CN π bond, and addition to N. It is seen from Figure 1 that the potential surface for abstraction of H is totally repulsive. Therefore, this reaction pathway is expected to have a potential barrier which is considerably high. The potential surface for insertion into CH also exhibits a repulsive character when the distance between $N(^2D)$ and $HCN(^1\Sigma)$ is large but a slightly attractive character when the distance is small. It is hence considered that, although insertion into CH also has a potential barrier, it may be significantly smaller than that for abstraction of H. A deep well is seen around the point $(X, Y) = (0.6, 1.4)$ or $(0.6, -1.4)$. It is expected that when $N(^2D)$ approaches the CN bond from the direction orthogonal to the HCN molecular axis, $N(^2D)$ is captured and stabilized in this well and a stable intermediate is produced. Although the reaction pathway for addition to CN may be energetically more favorable than abstraction of H and insertion into CH, it is seen from the figure that a small potential barrier still exists for addition to CN. A deeper well is seen on the molecular axis of HCN. It is expected that when $N(^2D)$ approaches N from the direction parallel to the HCN molecular axis, $N(^2D)$ is again captured and stabilized in this well and another stable intermediate is produced. The contour map shows that the potential surface for addition to N is totally attractive. Thus, comparison of the potential surfaces for the four reaction pathways has led us to conclude that, in the initial step of the $N(^2D) + HCN(^1\Sigma)$ reaction, $N(^2D)$ addition to N is the energetically most favorable pathway and $N(^2D)$ addition to the CN bond is the second. The present result can roughly be estimated from the viewpoint of orbital interaction. It was predicted that amplitudes of frontier orbitals, i.e., HOMO, LUMO, and next HOMO, etc., of HCN are localized around the CN bond; therefore, it is expected that $N(^2D)$ favorably approaches the N atom or CN bond of HCN. Although the present CASSCF(9,9) calculation yields a qualitative result, it provides useful information for understanding the global feature of the potential energy surface that cannot be described by theoretical methods based on single-reference HF theory.

B. Geometries and Energetics for Overall Reaction. The $N(^2D) + HCN(^1\Sigma)$ reactants produce stable intermediates right after the initial processes, and these intermediates undergo TSs and other intermediates before reaching final products. In this subsection, the computational results of overall reaction pathways except for the initial processes for the lowest doublet-state potential surface are reported. As compared to the potential surface for the initial processes discussed above, multiconfigurational character is not so significant for species in the middle stage; therefore, we employed the MP2 level of theory for geometry optimization and harmonic vbrational analyses and the PMP4 level for higher level single-point energy calculations. Optimized geometries obtained at the MP2(full)/cc-pVTZ level for minima and TSs are shown in Figures 2 and 3, respectively. Harmonic vibrational frequencies calculated at the same level of theory for these stationary points and several fragments relevant to the present reaction are summarized in Table 1. Total energies calculated at the MP2(full)/cc-pVTZ and PMP4-(SDTQ,full)/cc-pVTZ levels for the MP2(full)/cc-pVTZ geom-

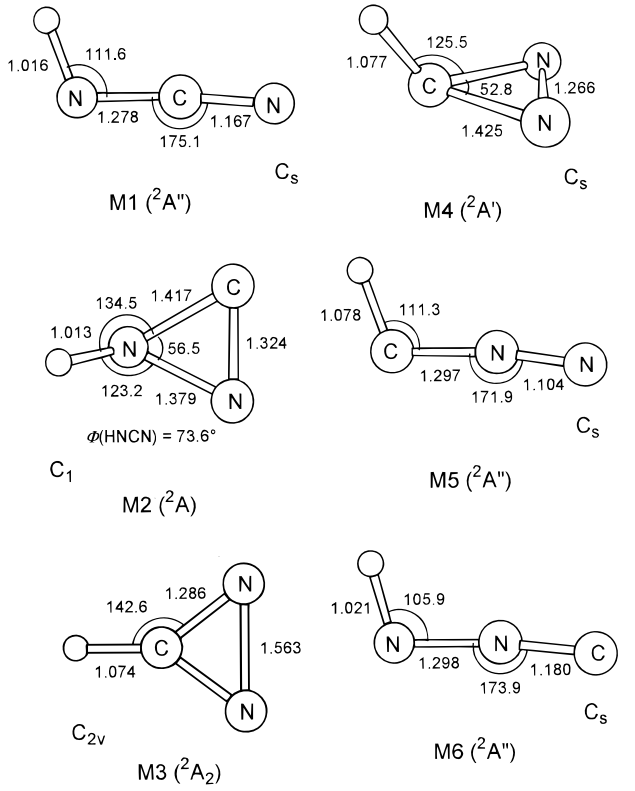

Figure 2. Optimized geometries for intermediates obtained at the MP2-(full)/cc-pVTZ level. Bond lengths and angles are given in Å and degrees, respectively.

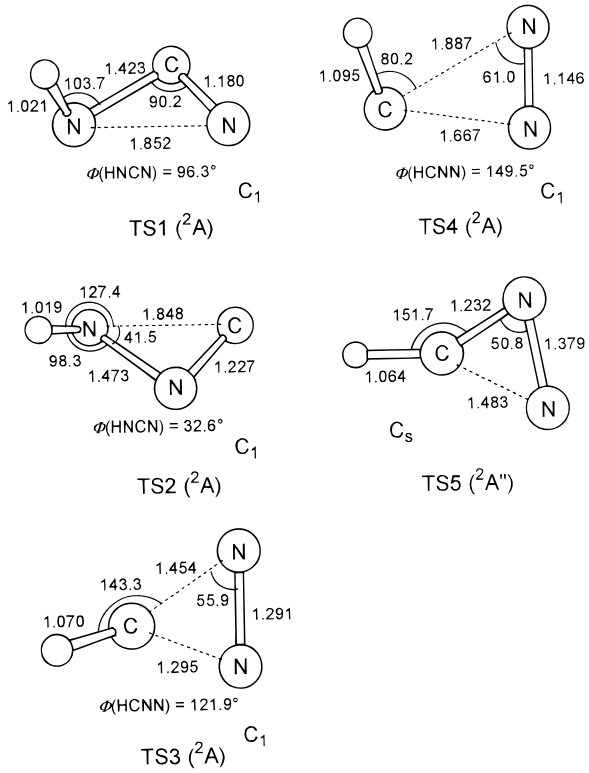

Figure 3. Optimized geometries for TSs obtained at the MP2(full)/cc-pVTZ level. Bond lengths and angles are given in Å and degrees, respectively.

TABLE 1: Harmonic Vibrational Frequencies Calculated at the MP2(full)/cc-pVTZ Level

molecule	sym	frequency/cm^{-1}					
		fragment					
N_2 ($^1\Sigma_g$)	$D_{\infty h}$	2218 (σ_g)					
CH ($^2\Pi$)	$C_{\infty v}$	2974 (σ)					
NH ($^3\Sigma$)	$C_{\infty v}$	3414 (σ)					
CN ($^2\Sigma$)	$C_{\infty v}$	2908 (σ)					
CNN ($^3\Sigma$)	$C_{\infty v}$	433 (π)	433 (π)	1072 (σ)	1723 (σ)		
NCN ($^3\Sigma_g$)	$D_{\infty h}$	530 (π_u)	530 (π_u)	951 (σ_u)	1376 (σ_g)		
HCN ($^1\Sigma$)	$C_{\infty v}$	727 (π)	727 (π)	2045 (σ)	3492 (σ)		
		intermediate (minimum)					
M1 ($^2A''$)	C_s	531 (a′)	551 (a″)	1009 (a′)	1169 (a′)	1899 (a′)	3562 (a′)
M2 (^2A)	C_1	608	834	1012	1146	1548	3527
M3 ($^2A_2$)	C_{2v}	696 (a1)	763 (b_2)	1048 (b_1)	1206 (b_2)	1747 (a_1)	3299 (a_1)
M4 ($^2A'$)	C_s	977 (a″)	1084 (a′)	1127 (a′)	1523 (a′)	1624 (a″)	3216 (a′)
M5 ($^2A''$)	C_s	584 (a″)	643 (a′)	946 (a′)	1204 (a′)	2736 (a′)	3286 (a′)
M6 ($^2A''$)	C_s	367 (a″)	395 (a′)	1052 (a′)	1383 (a′)	2251 (a′)	3473 (a′)
		transition state (saddle point)					
TS1 (^2A)	C_1	593*i*	623	861	1250	2380	3472
TS2 (^2A)	C_1	487*i*	342	814	1306	1897	3484
TS3 (^2A)	C_1	1355*i*	823	939	1116	1717	3316
TS4 (^2A)	C_1	489*i*	511	707	1279	2964	3111
TS5 ($^2A''$)	C_s	1525*i* (a′)	535 (a′)	927 (a′)	1232 (a′)	3035 (a′)	3477 (a′)

TABLE 2: Total Energy and Zero-Point Vibrational Energy (ZPE) for the MP2(full)/cc-pVTZ Geometries (hartree)

species	sym	MP2(full)	$\langle \mathbf{S}^2 \rangle^a$	ZPE	PMP4(SDTQ,full)
		fragment			
N (^4S)		−54.50681	0.376		−54.52447
N (^2D)		−54.44390	1.766		−54.43659
H (^2S)		−0.49981	0.75		−0.49981
N_2 ($^1\Sigma_g$)	$D_{\infty h}$	−109.38328	0.0	0.00505	−109.40625
CH ($^2\Pi$)	$C_{\infty v}$	−38.39360	0.759	0.00677	−38.41886
NH ($^3\Sigma$)	$C_{\infty v}$	−55.12973	2.015	0.00778	−55.15232
CN ($^2\Sigma$)	$C_{\infty v}$	−92.54133	0.993	0.00663	−92.58294
CNN ($^3\Sigma$)	$C_{\infty v}$	−147.18514	2.197	0.00834	−147.24464
NCN ($^3\Sigma_g$)	$D_{\infty h}$	−147.22248	2.364	0.00772	−147.29343
HCN ($^1\Sigma$)	$C_{\infty v}$	−93.28116	0.0	0.01593	−93.30789
		intermediate (minimum)			
M1 ($^2A''$)	C_s	−147.87756	0.919	0.01987	−147.93619
M2 (^2A)	C_1	−147.77056	0.817	0.01976	−147.82042
M3 ($^2A_2$)	C_{2v}	−147.81453	0.932	0.01995	−147.87295
M4 ($^2A'$)	C_s	−147.80562	0.765	0.02176	−147.84797
M5 ($^2A''$)	C_s	−147.82026	0.892	0.02141	−147.87651
M6 ($^2A''$)	C_s	−147.81946	0.817	0.02032	−147.87123
		transition state (saddle point)			
TS1 (^2A)	C_1	−147.75976	1.061	0.01956	−147.82470
TS2 (^2A)	C_1	−147.75874	0.779	0.01787	−147.81056
TS3 (^2A)	C_1	−147.77598	1.005	0.01802	−147.83797
TS4 (^2A)	C_1	−147.76458	0.797	0.01953	−147.81295
TS5 ($^2A''$)	C_s	−147.80111	0.784	0.02097	−147.84714

[a] The expectation value of spin operator $\mathbf{S}^2$ for the reference HF wave functions.

etries are given in Table 2. Also given in Table 2 are the expectation values of spin operator $\mathbf{S}^2$, $\langle \mathbf{S}^2 \rangle$, for the reference UHF wave function; $\langle \mathbf{S}^2 \rangle$ is thought to be a measure for the validity of the employed UHF wave function. Relative energies with respect to the N(^{4}S) + HCN($^1\Sigma$) asymptote obtained at the PMP4(SDTQ,full)/cc-pVTZ level, which includes the zero-point energy (ZPE) correction, are shown in Figure 4. We will discuss below the mechanisms of the overall reaction pathways starting with the following three initial processes: insertion into the CH bond, addition to the CN π bond, and addition to the N atom. In the last part of this subsection we will propose a N(^{2}D) quenching mechanism via the spin-forbidden process.

N(^{2}D) insertion into the CH bond may require some amount of energy to surmount the potential barrier, as discussed in the previous subsection, and lead to the production of an intermediate M1, which was predicted to be energetically the lowest minimum in the N(^{2}D) + HCN($^1\Sigma$) system. As shown in Figure 4, the relative energy of M1 was calculated to be −62.7 kcal mol^{-1}. Three reaction pathways from M1 can be considered: decomposition into NH($^3\Sigma$) + CN($^2\Sigma$), decomposition into H(^{2}S) + NCN($^3\Sigma_g$), and isomerization to the other intermediate. M1 decomposition into NH($^3\Sigma$) + CN($^2\Sigma$) is seen to be energetically unfavorable, since the NH($^3\Sigma$) + CN($^2\Sigma$) product channel was calculated to be 4.9 kcal mol^{-1} higher in energy than the N(^{2}D) + HCN($^1\Sigma$) reactants. M1 decomposition into H(^{2}S) + NCN($^3\Sigma_g$) is considered to be an energetically possible pathway, since the H(^{2}S) + NCN($^3\Sigma_g$) product channel was predicted to be 35.7 kcal mol^{-1} lower in energy than the N(^{2}D) + HCN($^1\Sigma$) reactants. It would be expected that a small barrier might exist for this decomposition, since during the NH bond scission two M1 CN bonds, which are originally single and triple bonds, change into two double bonds of the NCN molecule. This can be seen from the optimized bond lengths of M1 shown in Figure 2 and from the result that the CN bond length of the NCN molecule was optimized to be 1.209 Å. However, geometry optimization of the TS at the present MP2(full) level was unsuccessful. This is because this decomposition leads to the production of two open-shell species and high multiconfigurational character should occur in the electronic state of the TS. M1 isomerization into the other stable intermediate M2 is seen to occur more easily than the other two pathways. It should be noted, however, that although the TS for this isomerization, TS1, was obtained at the MP2(full)/cc-pVTZ level, it was estimated to be slightly lower in energy than M2 by the single-point energy calculation at the PMP4(SDTQ,full)/cc-pVTZ level. This is due to a considerably large spin contamination for TS1; as shown in Table 2, $\langle \mathbf{S}^2 \rangle$ for TS1 was estimated to be 1.061, which is the largest among all TSs obtained in the present calculation. It was found that M2 further isomerizes into the other intermediate M6 via TS2; the relative energies for TS2 and M6 were calculated to be 14.9 and −21.6 kcal mol^{-1}, respectively, at the PMP4(SDTQ,full)/cc-pVTZ level, including the ZPE correction. M6 can lead to mainly two product channels, NH($^3\Sigma$) + CN($^2\Sigma$) and H(^{2}S) + CNN($^3\Sigma$), but their relative energies were predicted considerably high and they are energetically unimportant. M6 decomposition into H(^{2}S) + CNN($^3\Sigma$) might have a TS for the same reason for M1 decomposition into H(^{2}S)

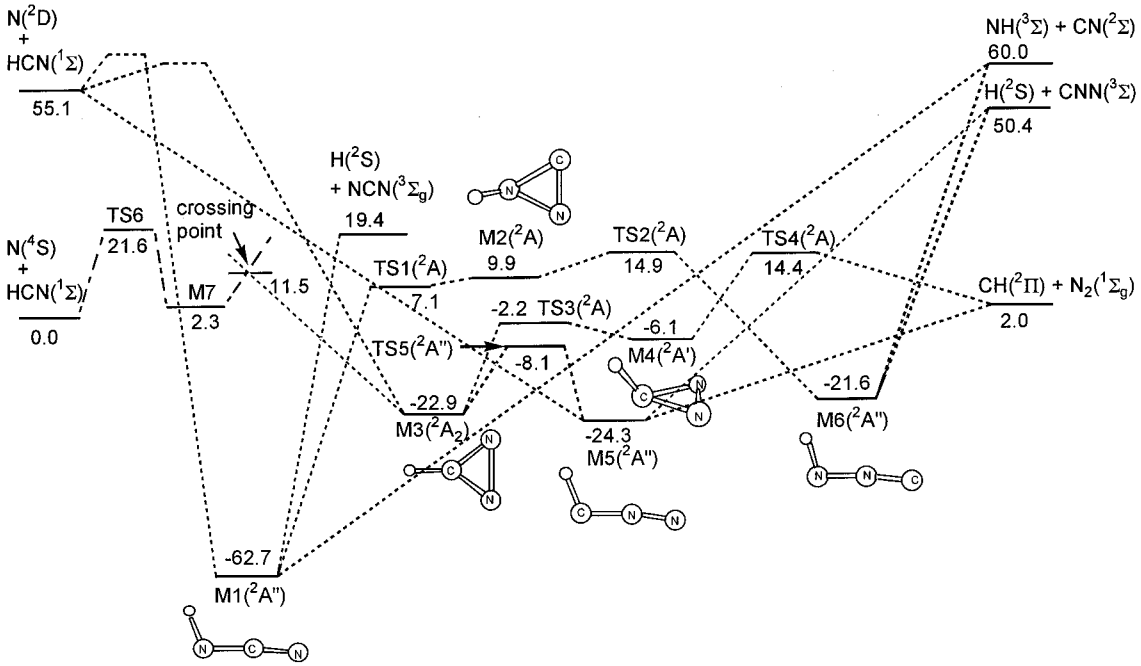

Figure 4. Dotted line represents relative potential energy for the lowest doublet state predicted at the PMP4(SDTQ,full)/cc-pVTZ//MP2(full)/cc-pVTZ level including the ZPE correction. Dashed−dotted line represents relative potential energy for the lowest quartet state taken from refs 31 and 32. The unit is kcal mol^{-1}.

+ NCN($^3\Sigma_g$); however, the TS was not optimized due to its unimportance for energetics.

N(^{2}D) addition to the CN π bond may require a small amount of energy to surmount the potential barrier, as discussed in the previous subsection, and lead to the production of an intermediate M3 with C_{2v} symmetry whose relative energy was computed to be −22.9 kcal mol^{-1}. There exist two isomerization pathways from M3 into the other intermediates M4 and M5. Isomerization into M4 via TS3 involves a symmetry change in electronic wave function; the electronic wave function of M3 is antisymmetric while that of M4 is symmetric with respect to the C_s plane of M4. This is possible since symmetry of TS3 was predicted to be C_1. M4 leads to the CH($^2\Pi$) + N$_2$($^1\Sigma_g$) products, which was calculated to be energetically the lowest product channel in the N(^{2}D) + HCN($^1\Sigma$) system, via TS4; the relative energies of TS4 and the CH($^2\Pi$) + N$_2$($^1\Sigma_g$) asymptote were calculated to be 14.4 and 2.0 kcal mol^{-1}, respectively. Isomerization into M5 via TS5 is seen to be easier than that into M4 via TS3; the relative energies of TS5 and M5 were computed to be −8.1 and −23.4 kcal mol^{-1}, which are lower than those of TS3 and M4. M5 can lead to both the H(^{2}S) + CNN($^3\Sigma$) and CH($^2\Pi$) + N$_2$($^1\Sigma_g$) product channels, but the production of CH($^2\Pi$) + N$_2$($^1\Sigma_g$) was predicted to be much easier. M5 decomposition into H(^{2}S) + CNN($^3\Sigma$) may have a TS for the same reasons for M1 decomposition into H(^{2}S) + NCN($^3\Sigma_g$) and for M6 decomposition into H(^{2}S) + CNN($^3\Sigma$); however, the TS was not examined either due to its unimportance for energetics. It is thought that M5 decomposition into CH($^2\Pi$) + N$_2$($^1\Sigma_g$) is a simple bond scission and does not have a barrier, since bond characters do not change during this process. This can be understood from the bond lengths for the optimized geometry of M5 shown in Figure 2.; the NN bond of M5 is seen to be a triple bond and the produced N$_2$ molecule has a triple bond.

N(^{2}D) addition to the N atom is briefly mentioned. This addition may have no potential barrier, as revealed in the previous subsection, and produces M5 whose decomposition processes were discussed above. It is seen that the reaction pathway, N(^{2}D) + HCN($^1\Sigma$) → M5 → CH($^2\Pi$) + N$_2$($^1\Sigma_g$), is the simplest and energetically most favorable pathway. It would sound more appropriate to refer to this pathway as N abstraction by N, since this process is so exothermic that the lifetime of M5 is quite short and the overall process can be seen as a simple abstraction of N.

The spin-forbidden reaction, CH($^2\Pi$) + N$_2$($^1\Sigma_g$) → N(^{4}S) + HCN($^1\Sigma$), has been extensively studied both experimentally and theoretically, since this reaction is known to be an important process in various fields of chemical research. We discuss here a mechanism of the N(^{2}D) quenching to N(^{4}S) via the spin-forbidden process using the quartet potential surface for the above reaction calculated by other authors.[31,32] In Figure 4 is also shown the quartet potential surface correlated to the N(^{4}S) + HCN($^1\Sigma$) asymptote. Relative energy values for M7 and TS6 are take from the result of Walch[32] and the value for the crossing point from that of Manaa and Yarkony.[31] Originally, these values are given relative to the CH($^2\Pi$) + N$_2$($^1\Sigma_g$) asymptote; hence in this figure 2.0 kcal mol^{-1}, which is the relative energy of CH($^2\Pi$) + N$_2$($^1\Sigma_g$) with respect to N(^{4}S) + HCN($^1\Sigma$) predicted in this work, is added to these original values. One sees from the figure that although the theoretical level for the quartet surface is different from the present one, the crossing point and TS6 are considerably lower in energy than the N(^{2}D) + HCN($^1\Sigma$) asymptote. It is therefore concluded that the quenching of N(^{2}D) to N(^{4}S) via intersystem crossing, i.e., N(^{2}D) + HCN($^1\Sigma$) → N(^{4}S) + HCN($^1\Sigma$), is an energetically feasible pathway.

C. Comparison to Other Calculations and Experiment. In Table 3 are given available theoretical and experimental data for the relative energies of the N(^{2}D) + HCN($^1\Sigma$) reaction. Although the available theoretical data obtained by other authors are quite limited, good agreement is seen between the present and G2M(RCC)[33] results. However, only the calculated relative energies of TS5, the TS for M3-M5 isomerization, are significantly different; TS5 obtained in this work is much lower in energy. The ICCI//CASSCF(11,11)/DZP result[32] shows qualitative agreement with the present result, but the ICCI method estimates the relative energies to be slightly higher. The CASSCF(11,11)/DZP and CASSCF(11,11)/TZ2P results[34] ex-

TABLE 3: Theoretical and Experimental Relative Energies for the N(^{2}D) + HCN Reaction System with respect to the CH($^2\Pi$) + N$_2$($^1\Sigma_g$) Asymptote (kcal mol^{-1})

	G2M(RCC)[a]	ICCI[b]	CAS[c]	CAS[d]	MRCI[e]	MRCI[f]	PMP4[g]	expt
CH($^2\Pi$) + N$_2$($^1\Sigma_g$)	0.0	0.0	0.0	0.0	0.0	0.0	0.0	0.0
N(^{2}D) + HCN($^1\Sigma$)							53.1	58.7
N(^{4}S) + HCN($^1\Sigma$)							−2.0	3.7
H(^{2}S) + NCN($^3\Sigma_g$)							17.4	23.3
H(^{2}S) + CNN($^3\Sigma$)							48.4	50.0
NH($^3\Sigma$) + CN($^2\Sigma$)							58.0	53.2
M1(^{2}A″)							−64.7	
M2(^{2}A)							7.9	
M3(^{2}A$_2$)	−23.5	−12.7	−9.1	−3.5	−12.1	−15.8	−24.9	
M4(^{2}A′)	−8.0	2.5					−8.1	
M5(^{2}A″)	−27.8		−13.0	−9.6	−23.9	−29.4	−26.3	
M6(^{2}A″)			−11.0				−23.6	
TS1(^{2}A)							5.1	
TS2(^{2}A)							12.9	
TS3(^{2}A)	−4.7	4.3					−4.2	
TS4(^{2}A)	10.8	18.2	23.8	28.5			12.4	
TS5(^{2}A″)	30.9						−10.1	
ref	33	32	34	34	34	34	this work	35

[a] The G2M(RCC)//B3LYP/6-311G(d,p) level with the ZPE correction. [b] The ICCI//CASSCF(11,11)/DZP level with the ZPE correction. [c] The CASSCF(11,11)/DZP level. [d] The CASSCF(11,11)/TZ2P level. [e] The MRCI(0.01)/TZ2P level. [f] The MRCI(0.01)/TZ2P level including Davidson's size-consistency correction. [g] The PMP4(SDTQ,full)/cc-pVTZ//MP2(full)/cc-pVTZ level including the ZPE correction.

TABLE 4: Optimized Bond Lengths and Angles for the Minima and TSs at Various Levels of Theory (Å and deg)

	NH	CN	CN	NN	CH	HNC	NCN	HCN	CNN	HNN	method
M1	1.017	1.281	1.168			113.1	175.0				MP2/6-311G(2df,2pd)[a]
	1.019	1.302	1.191			110.8	174.2				CCSD(T)/6-311G(2d,2p)[a]
	1.022	1.270	1.188			113.6	174.2				B3LYP/6-311++G(2df,p)[b]
	1.016	1.278	1.167			111.6	175.1				MP2(full)/cc-pVTZ[c]
M3		1.314	1.314	1.640	1.093		77.2	141.4			CAS(11,11)/TZ2P[d]
		1.324	1.324	1.635	1.080		76.3	141.9			CAS(11,11)/DZP[e]
		1.319	1.319	1.633	1.070		76.5	141.8			CAS(14,11)/6-31+G(d,p)[f]
		1.286	1.286	1.563	1.074		74.8	142.6			MP2(full)/cc-pVTZ[c]
M4		1.457	1.457	1.275	1.084		51.9	125.0			CAS(11,11)/DZP[e]
		1.454	1.454	1.269	1.074		45.2				CAS(14,11)/6-31+G(d,p)[f]
		1.425	1.425	1.266	1.077		52.8	125.5			MP2(full)/cc-pVTZ[c]
M5		1.311		1.153	1.076			113.2	168.0		CAS(11,11)/TZ2P[d]
		1.297		1.104	1.078			111.3	171.9		MP2(full)/cc-pVTZ[c]
M6	1.049	1.202		1.343					176.7	104.1	CAS(11,11)/DZP[d]
	1.021	1.180		1.298					173.9	105.9	MP2(full)/cc-pVTZ[c]
TS3		1.497	1.328	1.396	1.077		57.6	140.8			CAS(11,11)/DZP[e]
		1.454	1.295	1.291	1.070		55.7	143.3			MP2(full)/cc-pVTZ[c]
TS4		1.899	1.543	1.191	1.081		38.8	86.6			CAS(11,11)/DZP[d]
		1.925	1.515	1.214	1.093		39.1				CAS(11,11)/DZP[e]
		1.887	1.667	1.146	1.095		37.0	80.2			MP2(full)/cc-pVTZ[c]

[a] Reference 36. [b] Reference 37. [c] This work. [d] Reference 34. [e] Reference 32. [f] Reference 38.

hibit a large difference from the present result. This implies that dynamical electron-correlation effects should be included in the calculation in order to accurately estimate the relative energies. Although the MRCI(0.01)/TZ2P results[34] are quite limited, the relative energy of M5 is considerably improved. Experimental values,[35] which are available only for the asymptotic species, show relatively good agreement with the present result within a few kcal mol^{-1} s. This encourages us to believe that the present PMP4(SDTQ,full)/cc-pVTZ level of theory is reliable for estimating the relative energies of the present reaction system.

In Table 4 are summarized available theoretical data for geometries of minima and TSs in the N(^{2}D) + HCN($^1\Sigma$) system. As for the M1 geometry, a good agreement is seen between the present and other calculations. Since the MP2 electronic wave function for M1 is affected by a considerable amount of spin contamination, as shown in Table 2, it is desirable to compare to the result at the multiconfigurational level. Unfortunately, to our knowledge, there exists no calculated M1 geometry at the multiconfigurational level. Computational results at the CASSCF level are available for the intermediates M3-M6. It is seen that the present MP2(full)/cc-pVTZ level predicted the bond lengths to be slightly shorter than the CASSCF level. This is because dynamical electron-correlation effects are considered in the MP2 level, but not in the CASSCF level. Agreement between the present and other results for the M3-M6 geometries, however, seems quite good. Other theoretical results for the geometries of the TSs are available only for TS3 and TS4. The present MP2(full)/cc-pVTZ level again predicted the bond lengths to be slightly shorter than the CASSCF level except for one of the CN bonds in TS4. Agreement between the present and other results for the TS3 and TS4 geometries is again seen to be quite good. Although available data for calculated geometries based on other levels of theory are limited, the present comparison has led us to conclude that the MP2(full)/cc-pVTZ level can well predict the geometries of stationary points for the N(^{2}D) + HCN($^1\Sigma$) system.

4. Concluding Remarks

In this work ab initio MO calculations have been carried out for the N(^{2}D) + HCN($^1\Sigma$) reaction system. For initial processes,

due to the high multiconfigurational character, the CASSCF-(9,9)/cc-pVDZ level of theory was employed and the contour map for the potential energy surface as a function of the $N(^2D)$ position was drawn. It was found that addition of $N(^2D)$ to the N atom is energetically the most favorable pathway. Several intermediates and TSs located on overall $N(^2D) + HCN(^1\Sigma)$ reaction pathways except for the initial processes were optimized at the MP2(full)/cc-pVTZ level, and their single-point energies were calculated at the PMP4(SDTQ,full)/cc-pVTZ level. It was predicted that the main product channel is $CH(^2\Pi) + N_2(^1\Sigma_g)$, which is 53.1 kcal mol^{-1} lower in energy than the $N(^2D) + HCN(^1\Sigma)$ reactants. It was also found that the quenching of $N(^2D)$ to $N(^4S)$ via a spin-forbidden process is energetically feasible. Calculated geometries and energetics obtained in this work were compared to available theoretical and experimental data and agreement was found to be fairly good.

We believe that the present theoretical results are useful in understanding not only the chemistry of Titan's atmosphere but also that of other important processes including $N(^2D)$. Hopefully in the near future, experimental studies for the $N(^2D) + HCN(^1\Sigma)$ reaction will be undertaken in order to confirm the present theoretical predictions.

References and Notes

(1) Yung, Y. L.; Allen, M.; Pinto, J. P. *Astrophys. J.* **1984**, *55*, 465.

(2) Yung, Y. L. *Icarus* **1987**, *72*, 468.

(3) Lara, L. M.; Lellouch, E.; López-Moreno, J. J.; Rodrigo, R. *J. Geophys. Res.* **1996**, *101*, 23261.

(4) Fell, B.; Rivas, I. V.; McFadden, D. L. *J. Phys. Chem.* **1981**, *85*, 224.

(5) Umemoto, H.; Asai, T.; Kimura, Y. *J. Chem. Phys.* **1997**, *106*, 4985.

(6) Umemoto, H.; Kimura, Y.; Asai, T. *Chem. Phys. Lett.* **1997**, *264*, 215.

(7) Umemoto, H.; Kimura, Y.; Asai, T. *Bull. Chem. Soc. Jpn.* **1997**, *70*, 2951.

(8) Umemoto, H.; Nakae, T.; Hashimoto, H.; Kongo, K.; Kawasaki, M. *J. Chem. Phys.* **1998**, *109*, 5844.

(9) Umemoto, H.; Asai, T.; Hashimoto, H.; Nakae, T. *J. Phys. Chem. A* **1999**, *103*, 700.

(10) Alagia, M.; Balucani, N.; Cartechini, L.; Casavecchia, P.; Volpi, G. G.; Sato, K.; Takayanagi, T.; Kurosaki, Y., submitted for publication.

(11) Alagia, M.; Balucani, N.; Cartechini, L.; Casavecchia, P.; Volpi, G. G.; Pederson, L. A.; Schatz, G. C.; Lendvay, G.; Harding, L. B.; Hollebeek, T.; Ho, T.-S.; Rabitz, H. *J. Chem. Phys.* **1999**, *110*, 8857.

(12) Kurosaki, Y.; Takayanagi, T.; Sato, K.; Tsunashima, S. *J. Phys. Chem. A* **1998**, *102*, 254.

(13) Takayanagi, T.; Kurosaki, Y.; Sato, K.; Misawa, K.; Kobayashi, Y.; Tsunashima, S. *J. Phys. Chem. A* **1999**, *103*, 250.

(14) Takayanagi, T.; Kurosaki, Y.; Sato, K.; Tsunashima, S. *J. Phys. Chem. A* **1998**, *102*, 10391.

(15) Takayanagi, T.; Kurosaki, Y.; Misawa, K.; Sugiura, M.; Kobayashi, Y.; Sato, K.; Tsunashima, S. *J. Phys. Chem. A* **1998**, *102*, 6251.

(16) Kurosaki, Y.; Takayanagi, T. *J. Phys. Chem. A* **1999**, *103*, 436.

(17) Kobayashi, H.; Takayanagi, T.; Yokoyama, K.; Sato, T.; Tsunashima, S. *J. Chem. Soc., Faraday Trans.* **1995**, *91*, 3771.

(18) Kobayashi, H.; Takayanagi, T.; Tsunashima, S. *Chem. Phys. Lett.* **1997**, *277*, 20.

(19) Pederson, L. A.; Schatz, G. C.; Ho, T.-S.; Hollebeek, T.; Rabitz, H.; Harding, L. B.; Lendvay, G. *J. Chem. Phys.* **1999**, *110*, 9091.

(20) Takayanagi, T.; Kurosaki, Y. *J. Mol. Struct. (THEOCHEM)*, in press.

(21) Dupuis, M.; Watts, J. D.; Villar, H. O.; Hurst, G. J. B. HONDO Version 7, *Comput. Phys. Comm.* **1989**, *52*, 415.

(22) Frisch, M. J.; Trucks, G. W.; Schlegel, H. B.; Gill, P. M. W.; Johnson, B. G.; Robb, M A.; Cheeseman, J. R.; Keith, T.; Petersson, G. A.; Montgomery, J. A.; Raghavachari, K.; Al-Laham, M. A.; Zakrzewski, V. G.; Ortiz, J. V.; Foresman, J. B.; Cioslowski, J.; Stefanov, B. B.; Nanayakkara, A.; Challacombe, M.; Peng, C. Y.; Ayala, P. Y.; Chen, W.; Wong, M. W.; Andres, J. L.; Replogle, E. S.; Gomperts, R.; Martin, R. L.; Fox, D. J.; Binkley, J. S.; Defrees, D. J.; Baker, J.; Stewart, J. P.; Head-Gordon, M.; Gonzalez, C.; Pople, J. A. *Gaussian 94*, Revision D.3; Gaussian, Inc.: Pittsburgh, PA, 1995.

(23) Dunning, T. H., Jr. *J. Chem. Phys.* **1989**, *90*, 1007.

(24) Head-Gordon, M.; Pople, J. A.; Frisch, M. J. *Chem. Phys. Lett.* **1988**, *153*, 503.

(25) Frisch, M. J.; Head-Gordon, M.; Pople, J. A. *Chem. Phys. Lett.* **1990**, *166*, 275.

(26) Frisch, M. J.; Head-Gordon, M.; Pople, J. A. *Chem. Phys. Lett.* **1990**, *166*, 281.

(27) Head-Gordon, M.; Head-Gordon, T. *Chem. Phys. Lett.* **1994**, *220*, 122.

(28) Pople, J. A.; Binkley, J. S.; Seeger, R. *Int. J. Quantum Chem. Symp.* **1976**, *10*, 1.

(29) Krishnan R.; Pople, J. A. *Int. J. Quantum Chem.* **1978**, *14*, 91.

(30) Schlegel, H. B. *J. Chem. Phys.* **1986**, *84*, 4530.

(31) Manaa, M. R.; Yarkony, D. R. *Chem. Phys. Lett.* **1992**, *188*, 352.

(32) Walch, S. P. *Chem. Phys. Lett.* **1993**, *208*, 214.

(33) Morokuma, K.; Cui, Q.; Liu, Z. *Faraday Discuss.* **1998**, *110*, 71.

(34) Martin, J. M. L.; Taylor, P. R. *Chem. Phys. Lett.* **1993**, *209*, 143.

(35) *JANAF Thermochemical Tables*, 3rd ed.; National Standard Reference Data Service (U.S. National Bureau of Standards); U.S. GPO: Washington, D.C., 1985.

(36) Tao, F.-M.; Klemprer, W.; McCarthy, M. C.; Gottlieb, C. A.; Thaddeus, P. *J. Chem. Phys.* **1994**, *100*, 3691.

(37) Clifford, E. P.; Wenthold, P. G.; Lineberger, W. C.; Petersson, G. A.; Ellison, G. B. *J. Phys. Chem. A* **1997**, *101*, 4338.

(38) Gordon, M. S.; Kass, S. R. *J. Phys. Chem.* **1995**, *99*, 6548.